CHAPTER V
RESULTS AND DISCUSSION

Oxide films formed on samples were evaluated by both visual inspection and surface characterization techniques. The surface properties of the oxide films were characterized by using several surface characterization techniques. A Scanning Electron Microscope (SEM) was used to examine the morphology of the oxide films; Energy-Dispersive X-ray Analysis (EDXA) was used to determine the chemical composition of the oxide films. The chemical structure of the oxide films was identified by Raman Spectroscopy.

This study was focused on two parameters. The effects of coolant velocity and the time required for forming an oxide film on the oxide film properties. Therefore two sets of experiments were conducted. One is referred to as the static experiment (no flow or 0 m/s coolant velocity) and the other is referred to as the flow experiment (5 m/s coolant velocity). Each set of experiments was conducted with different exposure times. Moreover the bare metal samples – bare probe and bare coupon – were taken as a reference condition, with both time and coolant velocity zero, before filming occurs. Some samples from previous studies at CNER were used for comparison with the present study.

5.1 Visual Inspection

The preliminary characterization was done by visual inspection. Both visual surface image and surface color were observed obtaining the uniformity and the color of oxide films formed on the surface of carbon steel A106B.

5.1.1 Visual Surface Image of Samples

Figure 5.1 shows the visual surface images of a number of samples. It can be seen that there was a significant difference between the samples before and after filming especially for the coupon samples. The presence of a uniform and black surface was the oxide film formed. However, for the bare probe sample, Figure 5.1f,

the inner surface of the probe seems to have some oxide film on the surface before exposure

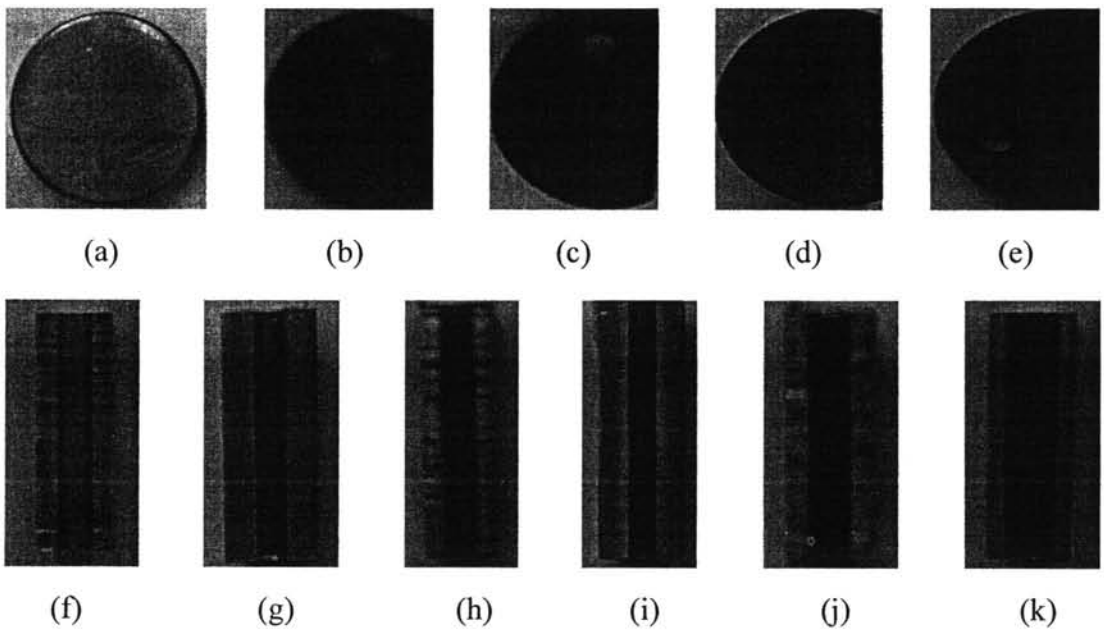

Figure 5.1 Visual surface images of samples (a) bare coupon sample (b) 0-m/s-15-day sample (c) 0-m/s-20-day sample (d) 0-m/s-30-day sample (e) 0-m/s-50-day sample (f) bare probe sample (g) 5-m/s-15-day sample (h) 5-m/s-38-day sample (i) 5-m/s-54-day sample (j) 10-m/s-38-day sample (k) 20-m/s-234-day sample.

5.1.2 Surface Color of Samples

The surface color of the samples is shown in Figure 5.2. Excluding the bare coupon sample, Figure 5.2a, the color of the oxide film formed on the surface is black. After comparing with the standard iron oxides color (Cornell, 2003), Figure B1, this oxide film was determined to be magnetite. However, this is only a preliminary observation using the visual technique. It must be confirmed by other surface characterizing techniques.

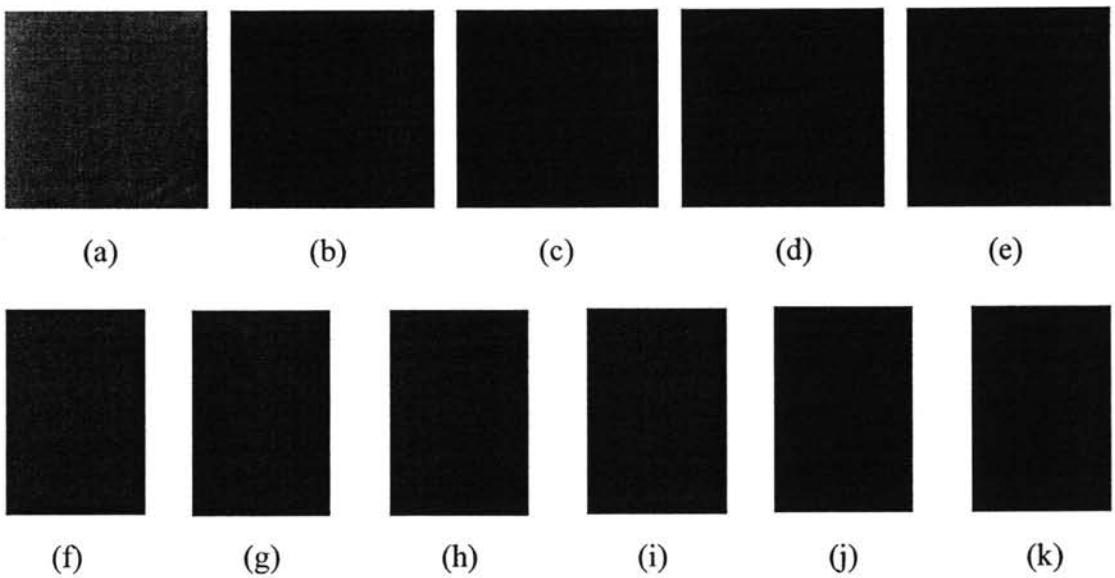

Figure 5.2 Visual surface color of samples (a) bare coupon sample (b) 0-m/s-15-day sample (c) 0-m/s-20-day sample (d) 0-m/s-30-day sample (e) 0-m/s-50-day sample (f) bare probe sample (g) 5-m/s-15-day sample (h) 5-m/s-38-day sample (i) 5-m/s-54-day sample (j) 10-m/s-38-day sample (k) 20-m/s-234-day sample.

5.2 Scanning Electron Microscope (SEM)

The surface morphology of the oxide films was characterized by the SEM technique. In this study, there are three results obtained by using this technique which are an SEM surface micrograph, SEM cross-sectional micrograph and Energy Dispersive X-ray Analysis (EDXA) data.

5.2.1 SEM Surface Micrographs

SEM micrographs of the surfaces were characterized. The static experiment and the flow experiment were separately discussed because of the difference in operating conditions. However, both experiments showed similar results in some cases.

5.2.1.1 Static Experiment

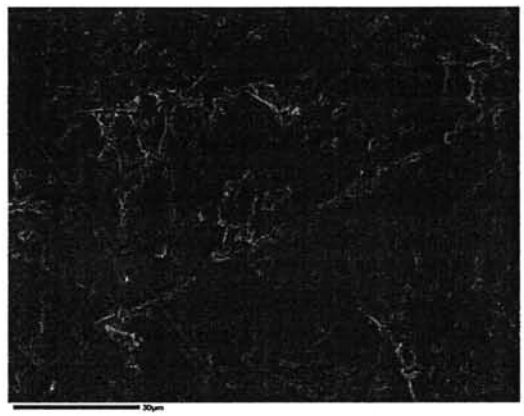

(a) 0 m/s, 0 day (Bare Coupon)

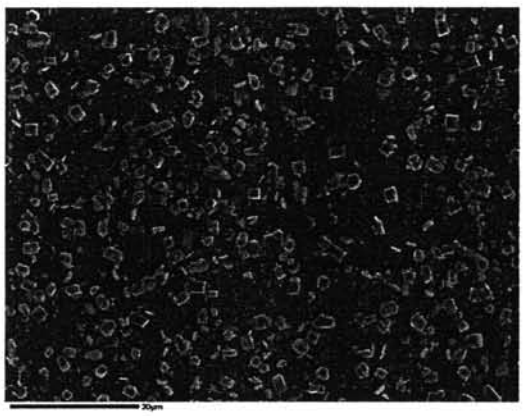

(b) 0 m/s, 15 days

(c) 0 m/s, 20 days

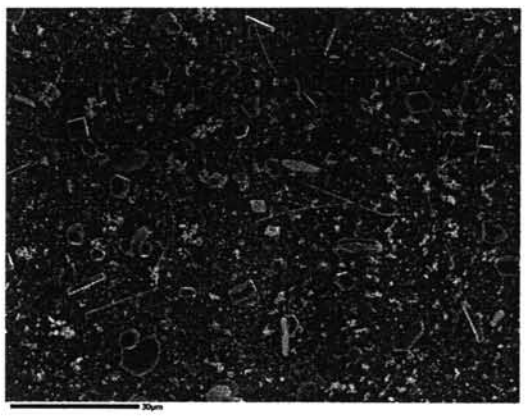

(d) 0 m/s, 30 days

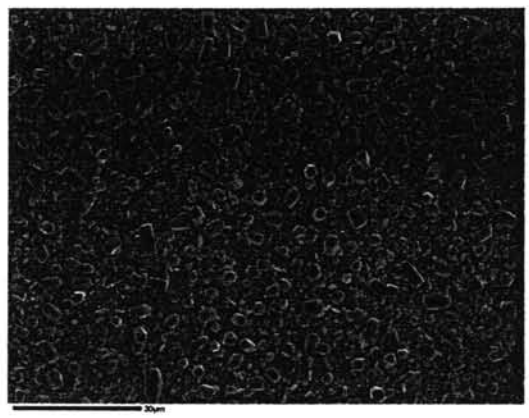

(e) 0 m/s, 50 days

Figure 5.3 SEM surface micrographs of oxide film formed under static condition with different exposure times at 1,000X magnification.

Figure 5.3 shows an SEM surface micrograph of the oxide film formed on metal under static conditions in an overview, 1,000X magnification. It is seen that the surface of the original metal (Figure 5.3a) was smoother than the surface of the sample after the film was formed (Figures 5.3b – 5.3e). The presence of crystalline particles was also found on the filmed samples. The image shows that longer exposure time gives higher amounts of crystalline paticles on the surface.

In order to investigate the surface in more detail it was necessary to increase the resolution of the micrographs. Figure 5.4 shows the oxide morphology at higher resolution, 10,000X magnification.

There are no oxide particles on the bare coupon surface, Figure 5.4a. The significantly different structure of the oxide particles can be seen in Figures 5.4b – 5.4e. Apparently there are two main types of oxide particles on the surface. One type is fine grain particles while the other type is hexagonal-shape crystalline particles which overlay the fine particles.

(a) 0 m/s, 0 day (Bare Coupon)

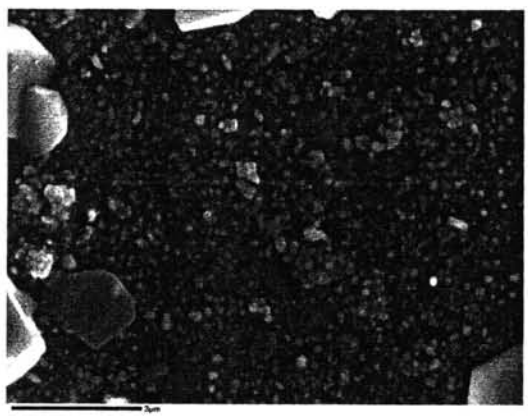

(b) 0 m/s, 15 days

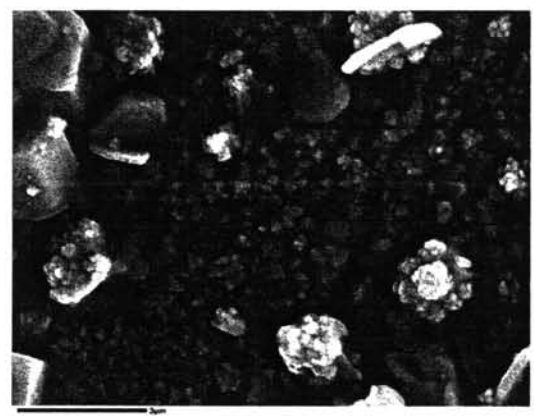

(c) 0 m/s, 20 days

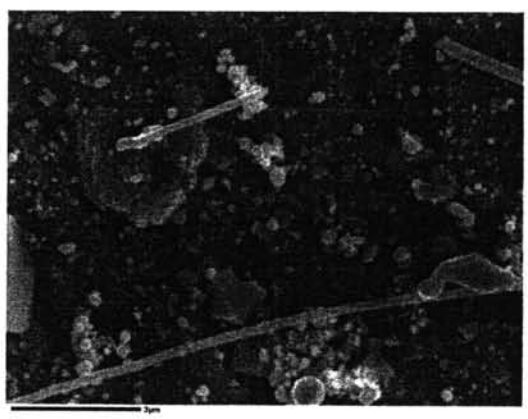

(d) 0 m/s, 30 days

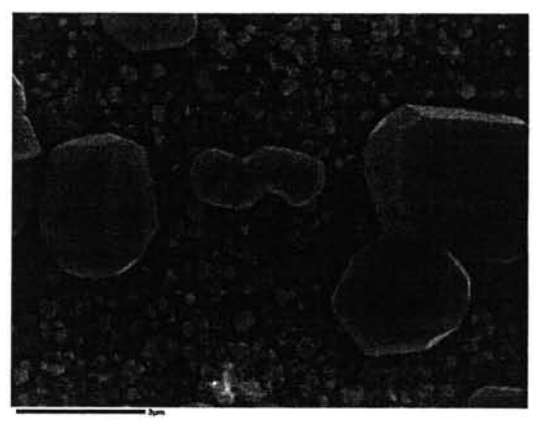

(e) 0 m/s, 50 days

Figure 5.4 SEM surface micrographs of oxide film formed under static condition with different exposure times at 10,000X magnification.

5.2.1.2 Flow Experiment

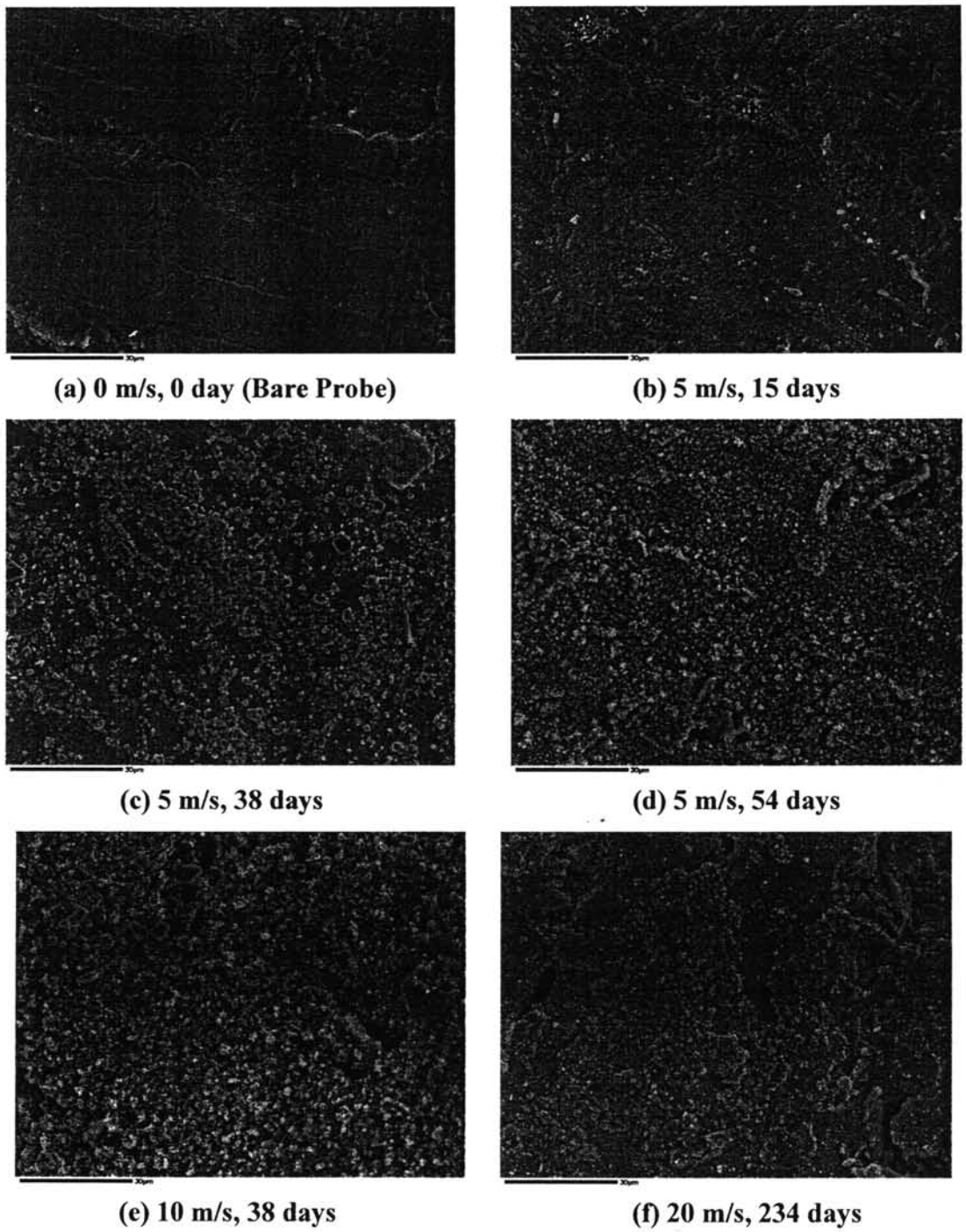

(a) 0 m/s, 0 day (Bare Probe)

(b) 5 m/s, 15 days

(c) 5 m/s, 38 days

(d) 5 m/s, 54 days

(e) 10 m/s, 38 days

(f) 20 m/s, 234 days

Figure 5.5 SEM surface micrographs of oxide film formed under flow condition with different exposure times and coolant velocities at 1,000X magnification.

The SEM surface micrograph of the oxide film formed on the metal surface under flow conditions in an overview, 1,000X magnification, is shown in Figure 5.5. A smoother surface was found for the bare metal probe sample, Figure 5.5a. It also shows that the particles overlaid the metal surface formed during the filming.

For 5-m/s samples, Figures 5.5b – 5.5d, the higher suface roughness – higher amounts of oxide particles formed – was observed in the longer exposure time sample. The 10-m/s sample (Figure 5.5e) seems to have the roughest surface. The surface of 20-m/s is not totally covered with the oxide particles. This could be caused by the high velocity coolant which flows over the surface and results in the dissolution or erosion of the oxide particles.

The oxide morphology at the higher resolution of micrographs, 10,000X magnification is shown in Figure 5.6. From Figure 5.6a it is seen that there was some oxide film on the metal surface before filming. However, this original oxide film was very thin and should not affect the formation of the oxide layer during the exposure

The morphology of other flow experiment samples show a significant difference from the bare metal sample. The presence of crystalline particles was observed on these samples, except 5-m/s-15-day and 10-m/s-38-day sample. However, the suface of both samples was different from the original metal surface. It can be concluded that there were two main types of oxide particles on the surface – fine grain particles and octahedral-shape crystalline particles.

The longer exposure time affected the amount and size of crystalline particles formed on the surface (5-m/s sample). However, based on the data from the SEM surface micrograph it cannot be concluded whether there is any effect on the fine grain particles.

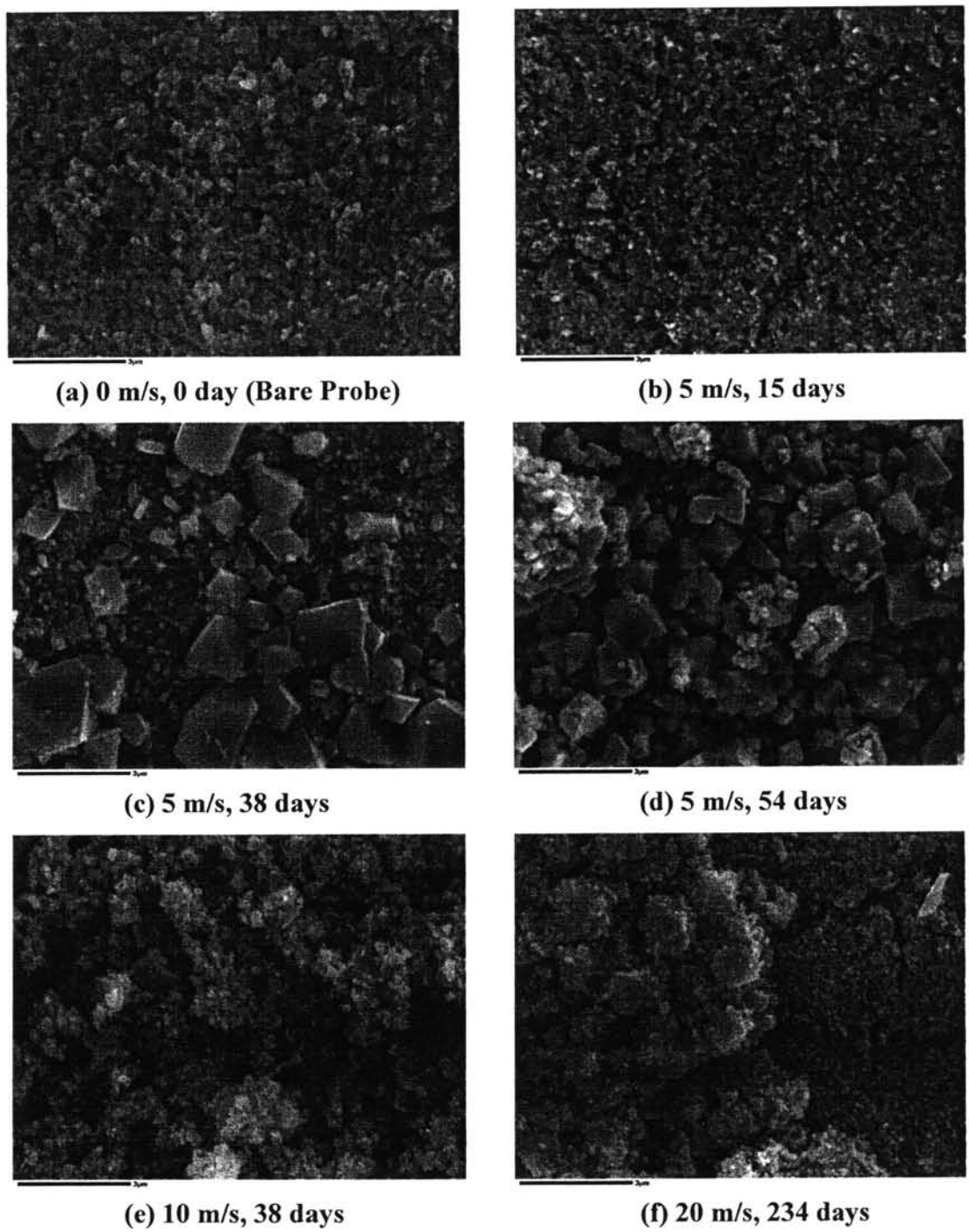

(a) 0 m/s, 0 day (Bare Probe)

(b) 5 m/s, 15 days

(c) 5 m/s, 38 days

(d) 5 m/s, 54 days

(e) 10 m/s, 38 days

(f) 20 m/s, 234 days

Figure 5.6 SEM surface micrographs of oxide film formed under flow condition with different exposure times and coolant velocities at 10,000X magnification.

5.2.2 SEM Cross-sectional Micrographs

In order to further study the oxide films the SEM cross-sectional micrographs of samples were obtained. Because of the difference in some system conditions, the static experiment and the flow experiment are separately discussed as this difference affected the oxide layers formed.

5.2.2.1 Static Experiments

Figure 5.7 shows the SEM cross-sectional micrographs of the oxide film formed on the metal surface under static conditions at 10,000X magnification. It is seen that there was no oxide layers on the bare metal sample (Figure 5.7a) while the oxide layers were observed on filmed samples. Although the surface of the base metals were not smooth, the oxide film formed was uniform and of consistent thickness along the metal surface.

As mentioned there were two main types of oxide particles on the surface. One was fine grain particles while the other particles were hexagonal-shape crystalline which overlay the fine particles. The oxide films observed on the metal surface from SEM cross-sectional micrographs were a layer of fine grain particles. Crystalline-shape particles were also found on the base layer, especially in Figure 5.7b, a hexagonal crystalline particle was clearly observed.

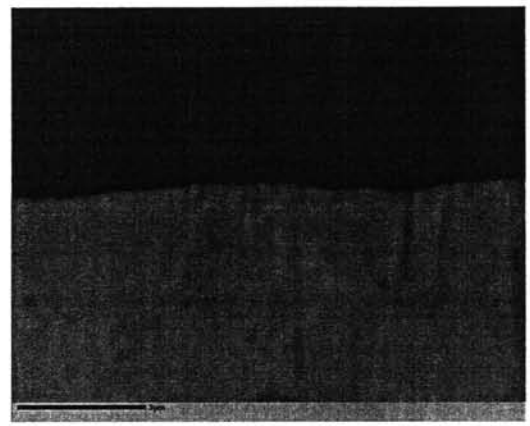

(a) 0 m/s, 0 day (Bare Metal)

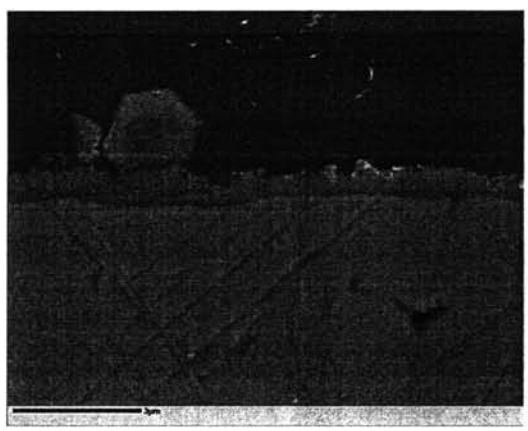

(b) 0 m/s, 15 days

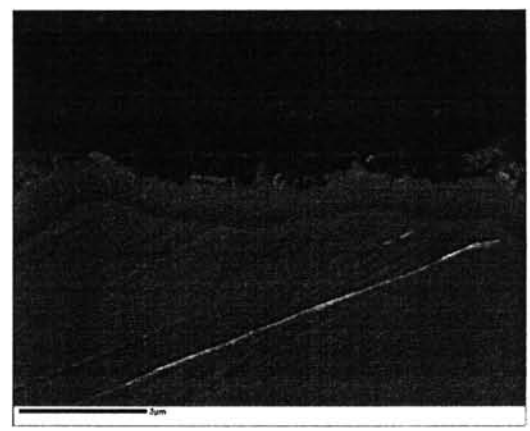

(c) 0 m/s, 20 days

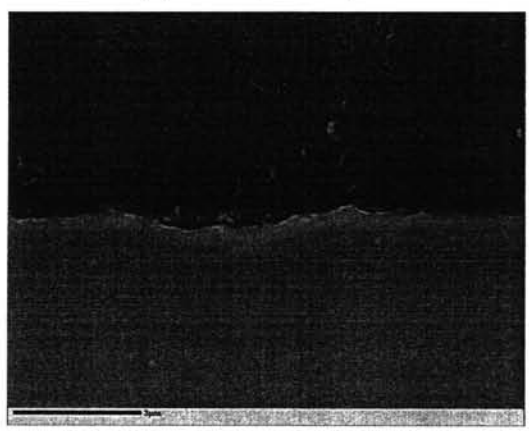

(d) 0 m/s, 30 days

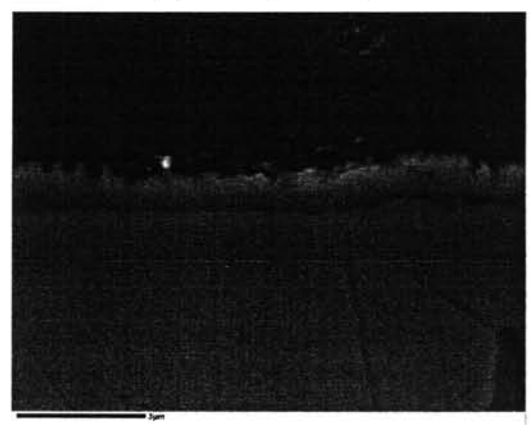

(e) 0 m/s, 50 days

Figure 5.7 SEM cross-sectional micrographs of oxide film formed under static condition with different exposure times at 10,000X magnification.

5.2.2.2 Flow Experiment

The SEM cross-sectional micrographs of the oxide film formed on the metal surface under flow conditions at 10,000X magnification are shown in Figure 5.8. The presence of oxide layers were found on the samples (Figure 5.8b – f) while there was no oxide layers on the bare metal sample (Figure 5.8a). The base metal surface of the samples were quite smooth except the 10-m/s-38-day sample which shows the uneven oxide films.

It is seen that there were two layers of oxide film – an inner layer and an outer layer. The inner layer has a higher packing density than the outer layer. The inner oxide layers observed were similar to the oxide layers formed on the static sample. However, there was only one oxide layer formed on 10-m/s-38-day sample. From the SEM suface micrograph of this sample (Figure 5.5e and 5.6e) the trace of the outer oxide layer appeared on the surface. The high velocity coolant could have an affect on the absence of this layer.

From the SEM surface micrograph there were two main types of oxide particles on the surface – fine grain particles and octahedral-shape crystalline particles. The oxide films seen on the metal surface from the SEM cross-sectional micrograph were the layer of fine grain particles. Also, some samples showed the presence of crystalline-shape particles on the base layer.

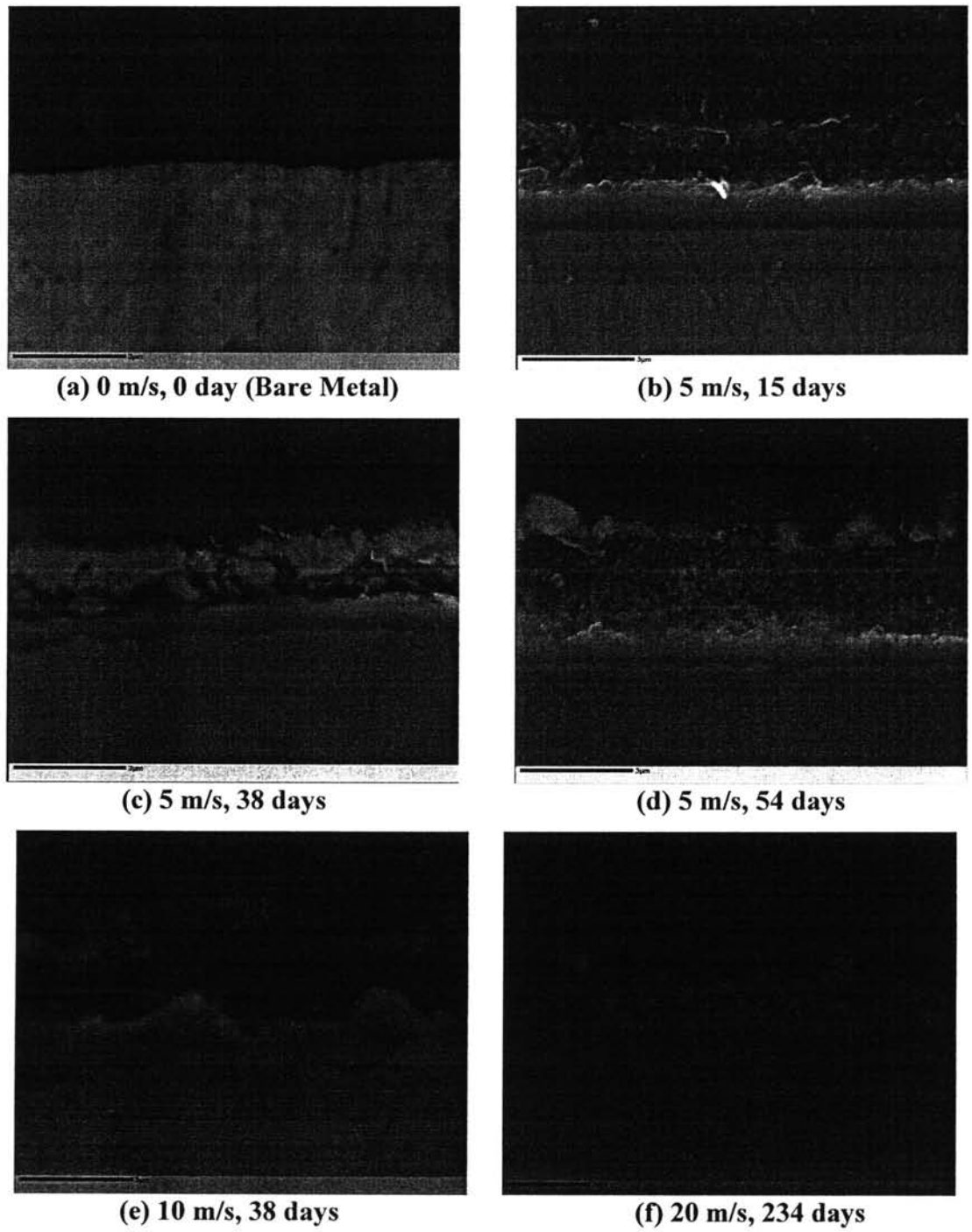

Figure 5.8 SEM cross-sectional micrographs of oxide film formed under flow condition with different exposure times and coolant velocities at 10,000X magnification.

5.2.3.2 Oxide Film Thickness Estimation

In order to compare the oxide films of all samples, a comparative SEM cross-sectional micrograph was constructed as shown in Figure 5.9.

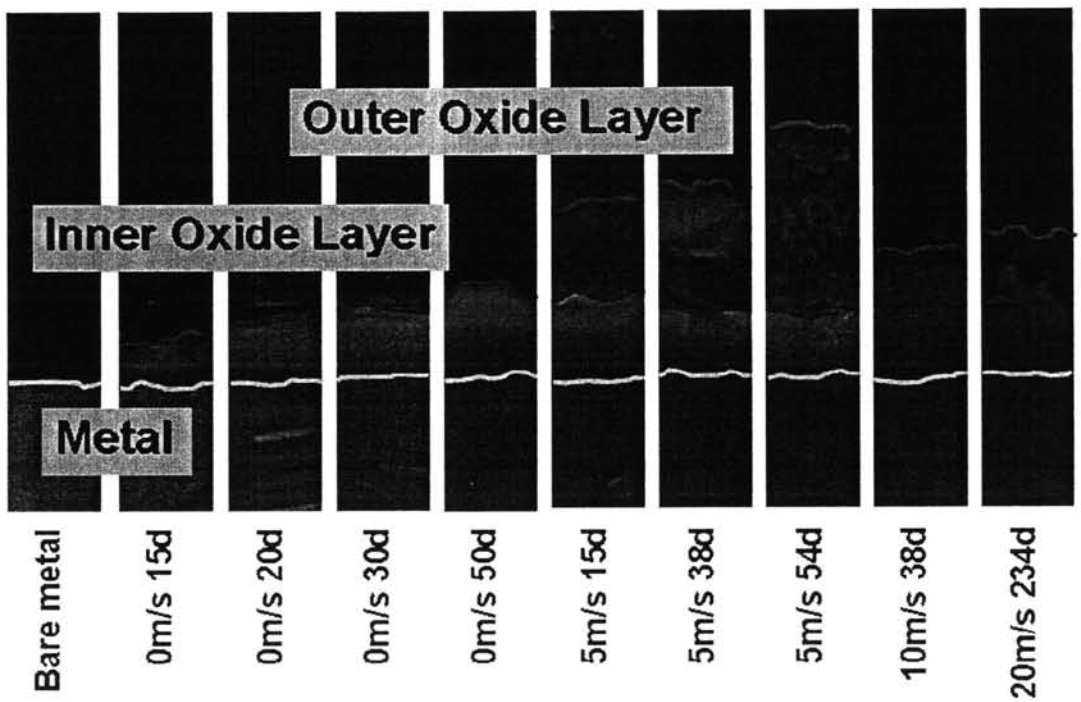

Figure 5.9 Comparative SEM cross-sectional micrographs of oxide films formed under static and flow conditions with different exposure times and coolant velocities at 10,000X magnification.

As discussed in the previous section, there was no oxide layers formed on the original bare metal. The 0-m/s samples showed only one layer of oxide film – this oxide layer referred to as inner oxide layer. From Figure 5.9 it can be seen that the longer exposure time resulted in a thicker oxide film formed on the surface. For 5-m/s samples, the presence of an outer oxide layer was observed. The thickness of the inner oxide layer was not significantly different whereas the thickness of the outer oxide layer changed with the exposure time. The longer exposure time gave a thicker outer oxide layer.

The oxide film of the 10-m/s sample was already discussed. Additionally the thickest inner oxide layers might because by the combination between both inner and outer oxide layers. Since the outer oxide layers were eroded or dissolved into the solution, the morphology of the outer layers was changed. Then the cross-sectional micrograph might give a similar result.

The 20-m/s sample was filmed under the highest coolant velocity so it should show a similar result to the 10-m/s sample. However, it showed two layers oxide. This could be caused from the long exposure time. When oxide particles are eroded or dissolved into the solution it can change the system to saturated condition with iron. This can lead to the precipitation of crystalline particles back to the surface.

From SEM cross-sectional micrographs the oxide film thickness can be roughly estimated as shown in Figure 5.10a. A Flow-Accelerated Corrosion (FAC) model is being developed by researchers at the University of New Brunswick in order to predict FAC in the plant. This work used the model developed by Silpsrikul (2007) which was 16 m/s coolant velocity as one of the conditions, the plant coolant velocity. By changing some parameters to fit with the experimental conditions in the laboratory, this model is used to calculate the oxide film thickness (Figure 5.10b) for comparison with the data obtained from the experiment.

Although the thickness from both methods was significantly different, the trend of the oxide film thickness between each group of samples was the same. Because this model is being developed for the plant condition, which operates under high velocity coolant, some equations or parameters are not be appropriate for the laboratory conditions. The adjustment of those equations and parameters is required in order to fit this model with the experimental data.

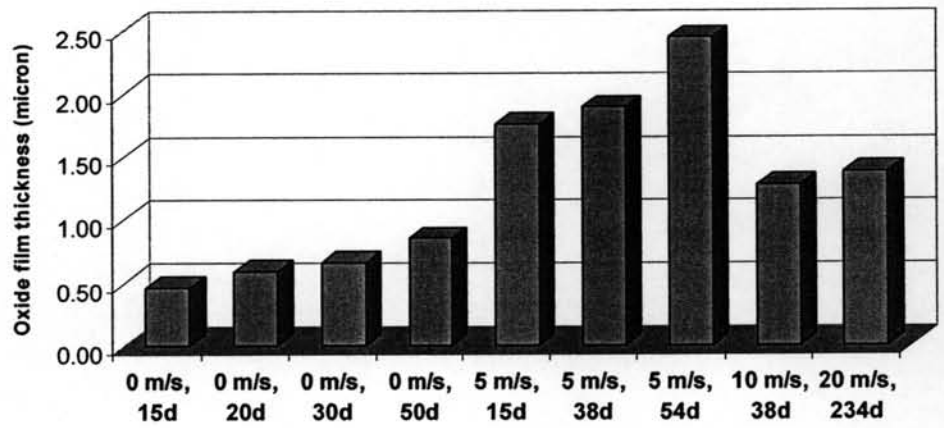

(a) The experiment

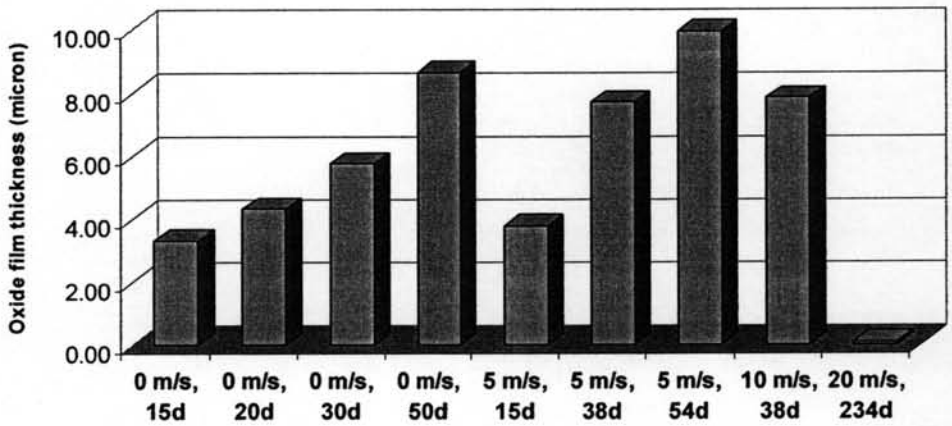

(b) The FAC Model

Figure 5.10 Oxide film thickness of the oxide layers obtained from (a) the experiment and (b) the FAC model.

5.2.3 Energy-Dispersive X-ray Analysis (EDXA)

Elemental analysis of samples were obtained by using EDXA coupled with SEM surface micrographs – in order to select the area for analysis. This analysis was performed on both bare samples and filmed samples. Both static and flow experiments showed two types of oxide particles – fine grain particles and crystalline particles. However, the crystalline particles had different shapes; octahedral and

hexagonal. In order to investigate the elemental composition, each type of crystalline particles were seperately analyzed.

5.2.2.1 Bare Metal Sample

Figure 5.11 illustrates the selected area of samples which were used for EDX analysis. The elemental analysis results of two bare metal samples are shown in Table 5.1. It is seen that the bare metal samples – bare coupon and bare probe – mainly consisted of iron (Fe). There were trace amounts of silicon (Si) and manganese (Mn) found on the surfaces. From the chemical composition of carbon steel these elements were part of its composition. The amounts of other elements such as phosphorous (P), sulfur (S), chromium (Cr) were low, less than 0.04%, so there were no signals of these elements from EDX spectrum.

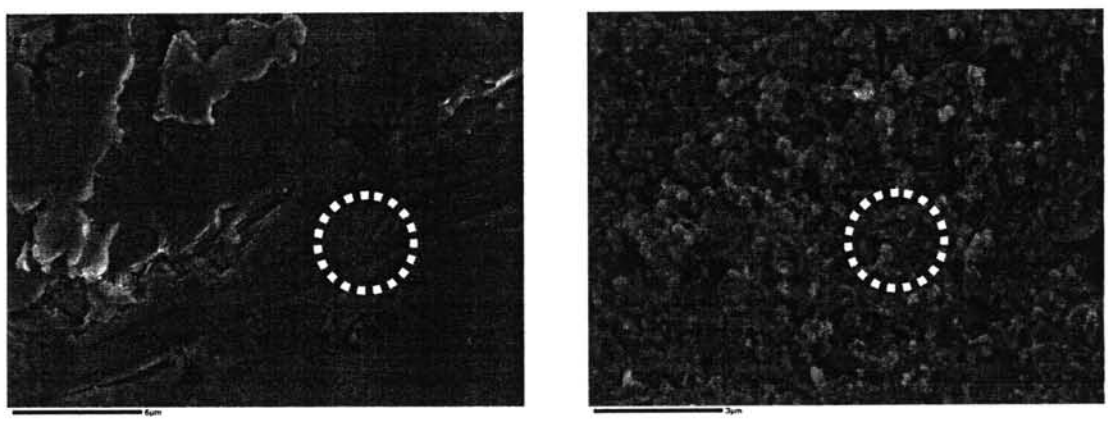

(a) Bare Coupon **(b) Bare Probe**

Figure 5.11 Selected area of bare metal samples for EDX analysis on SEM surface micrograph at 10,000X magnification.

Table 5.1 Elemental analysis of bare metal samples

Sample	Fraction (At %)			
	Fe	Si	Mn	Total
Bare Coupon	97.72	1.42	0.86	100.00
Bare Probe	98.46	0.77	0.77	100.00

5.2.2.2 Fine Grain Particles

The selected area of fine grain particles are shown in Figure 5.12. From EDX analysis (Figure 5.13), there were two main components in these particles, iron (Fe) and oxygen (O). The concentration of other components (Table C1) was low, so the concentration of those elements are not shown in Figure 5.13. The comparison of Fe:O ratio between each samples showed the consistent ratio, except 0-m/s-20-day sample. It can be concluded that these fine grain particles had an identical chemical structure.

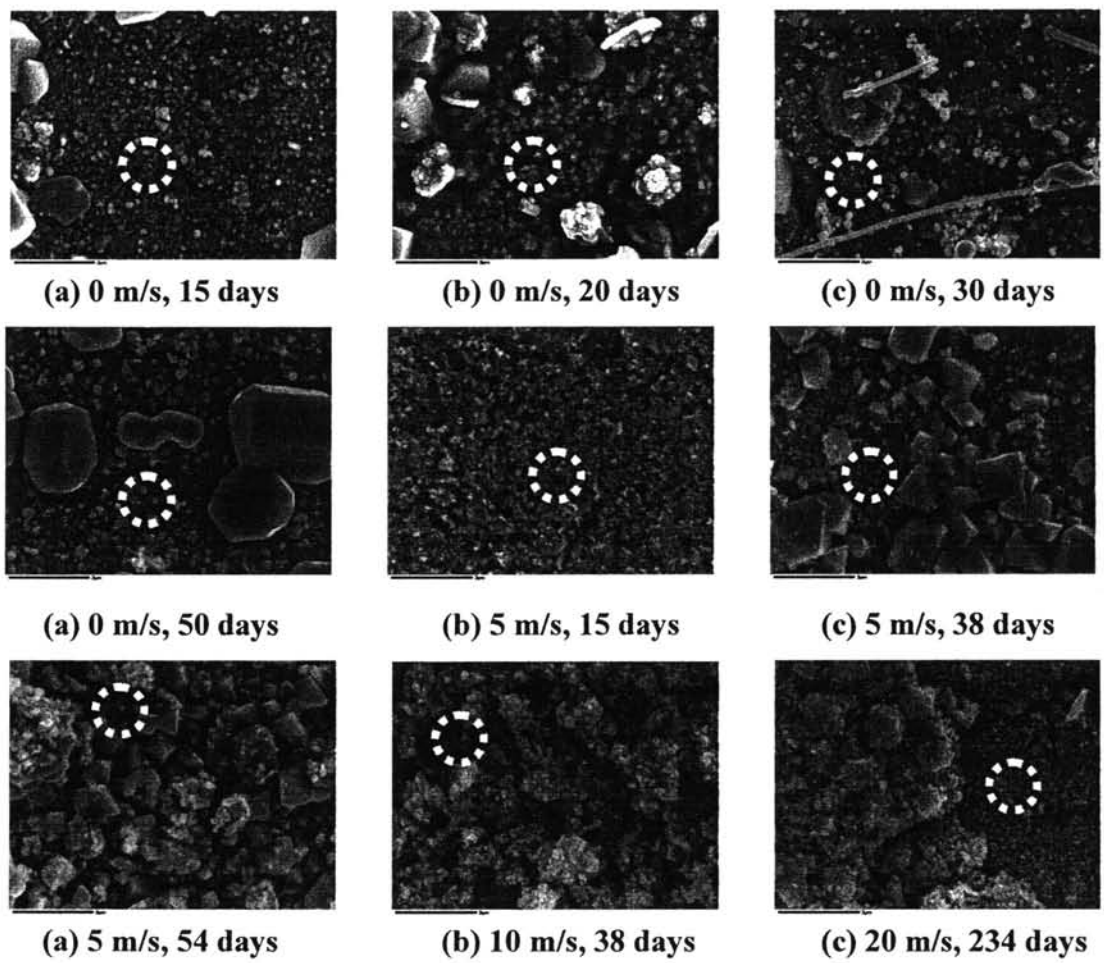

Figure 5.12 Selected fine grain particle areas of samples for EDX analysis on SEM surface micrograph at 10,000X magnification.

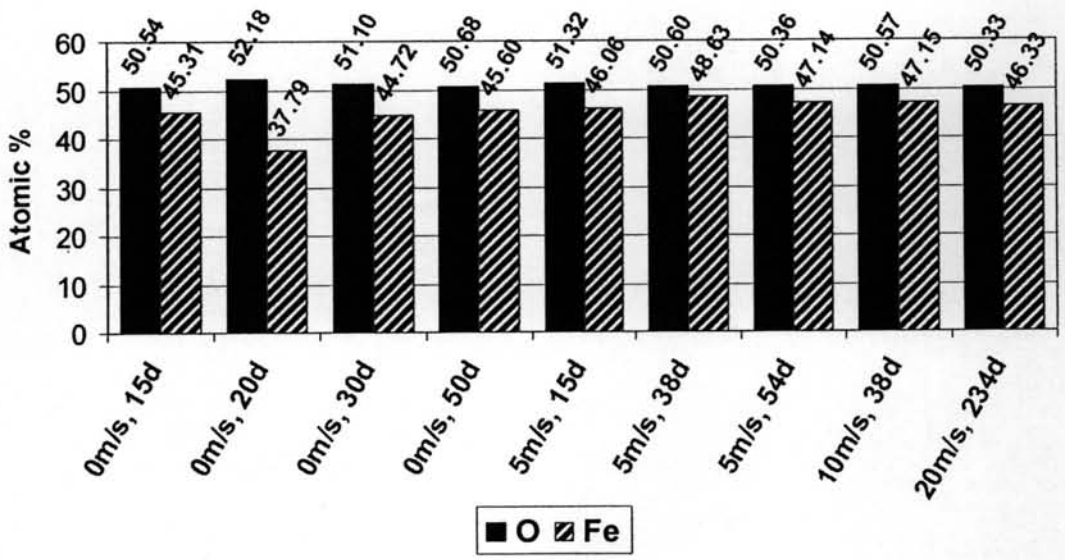

Figure 5.13 Elemental analysis of fine grain particles on samples.

When normalizing the concentration of some elements (Fe, Ni and Cr) relative to oxygen, the crystal structure of the oxide film could be roughly determined. Because the oxide particles might be magnetite (Fe_3O_4), so the concentration of oxygen was set to 4. Table 5.2 shows the ratio of Fe, Ni and Cr to O concentration. It is seen that the ratio of those elements was not close to 3 as assumed. Because of the thin oxide films, the EDX beam could pick up an interference signal from the underlying steel matrix, which mainly consisted of Fe. This Fe signal can affect the ratio of Fe:O by increasing the concentration of Fe in the oxide films. However, this method is used for elemental analysis. It can not determine the crystal structure. The crystal structure of oxide particles was analyzed by using another technique.

Table 5.2 Normalized concentration of Fe, Ni, and Cr to O ratio (fine grain particles)

Sample	Fraction (At %)					Normalized to O ratio				
	O	Fe	Ni	Cr	Total	O	Fe	Ni	Cr	Total
0 m/s, 15 days	50.54	45.31	0.00	0.00	95.85	4.00	3.59	0.00	0.00	7.59
0 m/s, 20 days	52.18	37.79	0.07	0.04	90.08	4.00	2.90	0.01	0.00	6.91
0 m/s, 30 days	51.10	44.72	0.00	0.06	95.87	4.00	3.50	0.00	0.00	7.51
0 m/s, 50 days	50.68	45.60	0.00	0.02	96.30	4.00	3.60	0.00	0.00	7.60
5 m/s, 15 days	51.32	46.06	0.00	0.10	97.48	4.00	3.59	0.00	0.01	7.60
5 m/s, 38 days	50.60	48.63	0.00	0.02	99.25	4.00	3.84	0.00	0.00	7.85
5 m/s, 54 days	50.36	47.14	1.57	0.04	99.12	4.00	3.74	0.12	0.00	7.87
10 m/s, 38 days	50.57	47.15	0.36	0.13	98.21	4.00	3.73	0.03	0.01	7.77
20 m/s, 234 days	50.33	46.33	2.41	0.05	99.12	4.00	3.68	0.19	0.00	7.88

5.2.2.3 Octahedral Crystalline Particles

Octahedral crystalline particles were found on some samples of flow experiments. When analyzing the selected area, Figure 5.14, the chemical composition of this type of particles is shown in Figure 5.15. It can be seen that there were two main elements in this crystals, oxygen and iron. The trace amounts of nickel (Ni) were found in two samples. The Ni contamination could come from the Hastelloy autoclave, which is a part of loop component. The presence of nickel could change the oxide type from magnetite to nickel ferrite by replacing iron atom in magnetite.

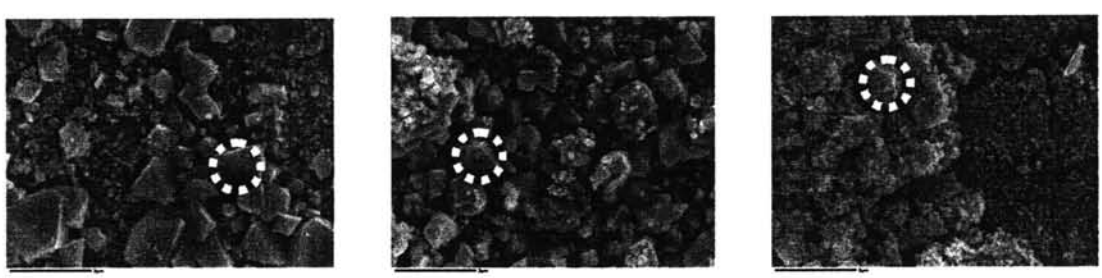

(a) 5 m/s, 38 days **(b) 5 m/s, 54 days** **(c) 20 m/s, 234 days**

Figure 5.14 Selected octahedral crystalline particle areas of samples for EDX analysis on SEM surface micrograph at 10,000X magnification.

Table 5.3 shows the normalized concentration of some elements (Fe, Ni and Cr) relative to oxygen. Magnetite has an octahedral shape crystal so the oxide particles could be magnetite (Fe_3O_4). Therefore, the concentration of oxygen was set to 4 and normalized the concentration of other elements relative to oxygen. It is seen that the ratio of those elements was not close to 3 as expected. As explained in fine grain particles section, the signals from the underlying Fe can affect on the results.

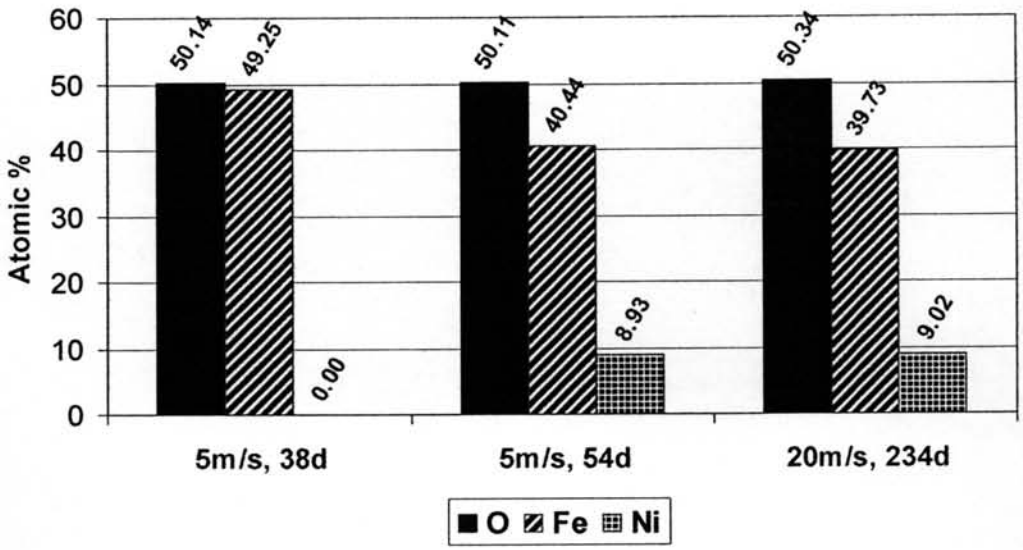

Figure 5.15 Elemental analysis of octahedral crystalline particles on samples.

Table 5.3 Normalized concentration of Fe, Ni, and Cr to O ratio (octahedral crystalline particles)

Sample	Fraction (At %)					Normalized to O ratio				
	O	Fe	Ni	Cr	Total	O	Fe	Ni	Cr	Total
5 m/s, 38 days	50.14	49.25	0.00	0.02	99.41	4.00	3.93	0.00	0.00	7.93
5 m/s, 54 days	50.11	40.44	8.93	0.10	99.57	4.00	3.23	0.71	0.01	7.95
20 m/s, 234 days	50.34	39.73	9.02	0.16	99.25	4.00	3.16	0.72	0.01	7.89

5.2.2.4 Hexagonal Crystalline Particles

All static experiment samples showed the hexagonal crystalline particles laid on fine grain particles. The EDX technique was used to analyze the elemental composition of these crystalline particles in the selected areas as shown in Figure 5.16. Figure 5.17 shows the chemical composition of the crystals. The result was different from the previous results – fine grain particles and octahedral crystalline particles. Three main components were found, oxygen (O), iron (Fe) and titanium (Ti). Because the autoclave used in the experiment is titanium, it could yield Ti in the solution, which can affect the type of crystal formed on the surface.

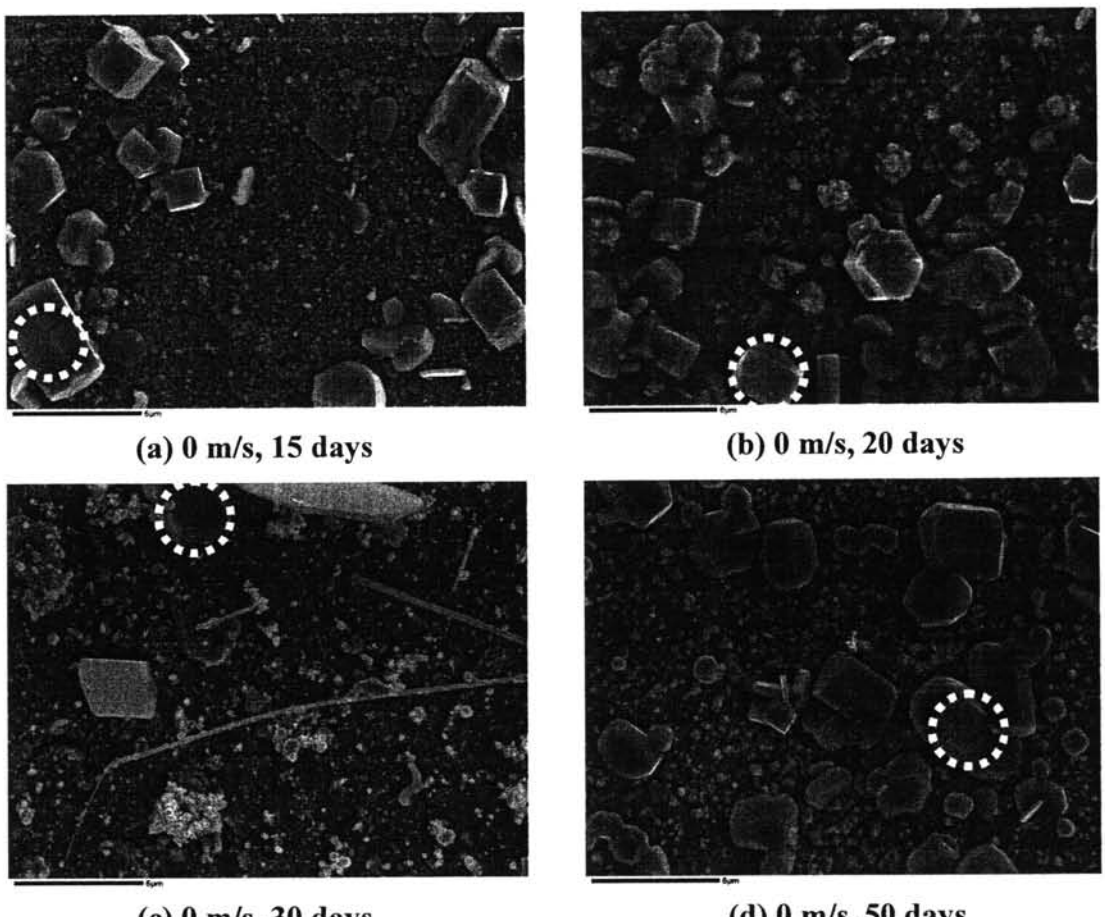

(a) 0 m/s, 15 days **(b) 0 m/s, 20 days**

(c) 0 m/s, 30 days **(d) 0 m/s, 50 days**

Figure 5.16 Selected hexagonal crystalline particle areas of samples for EDX analysis on SEM surface micrograph at 5,000X magnification.

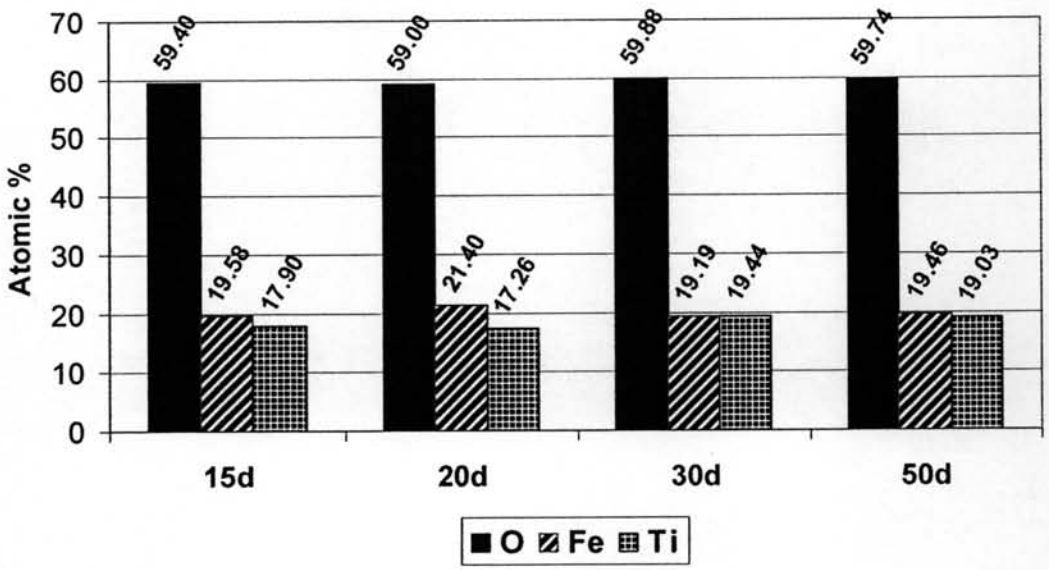

Figure 5.17 Elemental analysis of hexagonal crystalline particles on samples.

From the Fe-Ti-O system, there is one chemical compound that consists of the equal atomic concentration of iron and titanium which is ilmenite ($FeTiO_3$). This chemical compound has hexagonal shape crystal. Based on the results in Figure 5.17 and the shape of crystal observed, this hexagonal crystalline particle could be ilmenite.

The concentration of Fe and Ti were normalized relative to oxygen by setting the concentration of oxygen to 3. Table 5.4 shows the normalized result. It shows that the normalized concentration of both Fe and Ti are close to 1, so the crystalline particles formed under static condition could be ilmenite. However, as mentioned this technique cannot be used to determine the chemical structure of the compound. It is only a roughly estimation which has to be proved by another characterization technique.

Table 5.4 Normalized concentration of Fe and Ti to O ratio (hexagonal crystalline particles)

Sample	Fraction (At %)				Normalized to O ratio			
	O	Ti	Fe	Total	O	Ti	Fe	Total
0 m/s, 15 days	59.40	17.90	19.58	96.88	3.00	0.90	0.99	4.89
0 m/s, 20 days	59.00	17.26	21.40	97.66	3.00	0.88	1.09	4.97
0 m/s, 30 days	59.88	19.44	19.19	98.51	3.00	0.97	0.96	4.94
0 m/s, 50 days	59.74	19.03	19.46	98.24	3.00	0.96	0.98	4.93

From SEM surface micrographs at low magnification, 1,000X, as shown in Figure 5.3 and Figure 5.5, it can be seen that the hexagonal crystalline particles can be observed at this low magnification. It means the size of this crystal is larger than octahedral crystalline particles and also fine grain particles. Therefore when using EDX analysis, the EDX beam did not pick up the interference signals from the underlying steel matrix as much as those two types of particles. This leads to more precise results.

5.3 Raman Spectroscopy

The chemical structure of the oxide films can be identified by Raman Spectroscopy. When the sample surfaces were subjected to a laser beam, the raman spectrum for each sample was obtained. The comparison between each raman spectrum is shown in Figure 5.18. There are two patterns of spectrum; the first pattern is the spectrum of bare metals and the second pattern is the spectrum of filmed samples. It can be seen that the spectra of bare metals showed no peak over this raman shift range while the raman spectra of filmed samples showed one main peak at 660 – 680 cm^{-1}.

When compared with the reference magnetite spectrum (Figure 5.18), it can be concluded that the oxide films formed mainly consisted of magnetite and this chemical compound was formed after filming – because of the absence of peak in bare metal samples. Due to the trace amounts of other contaminants in each sample, the position of the peak could be shifted from the reference position.

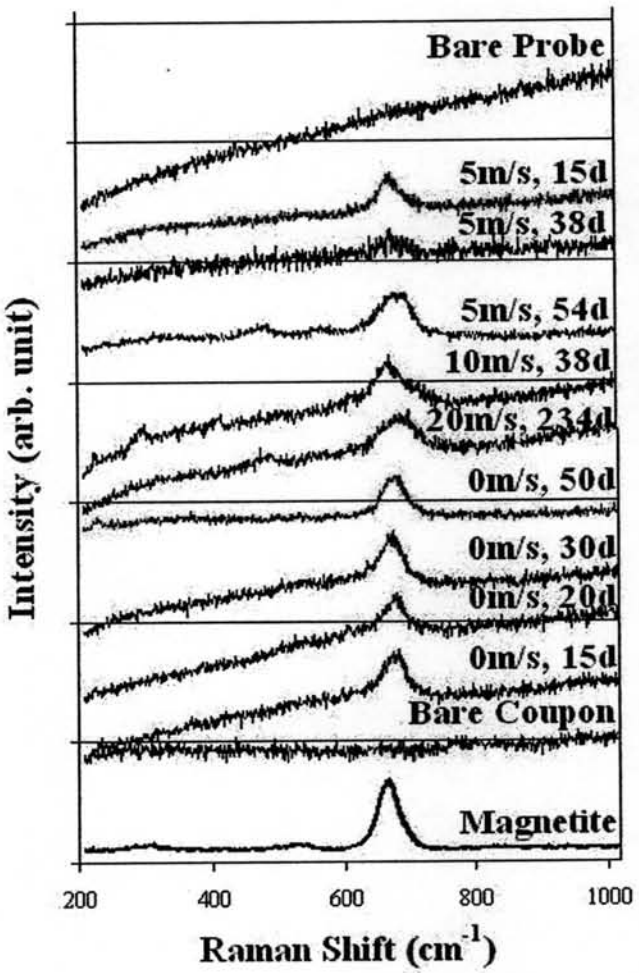

Figure 5.18 Raman spectra of samples compared with the reference magnetite spectrum.

There was no difference of spectrum for flow experiments after varying the analyzing spot. However, for static experiments some samples showed the different patterns of raman spectrum after pointing the laser beam onto the crystals on the surface as shown in Figure 5.19. Although the major peak is quite closed to the magnetite peak, the presence of minor peak at 370 – 375 cm^{-1} can be an indication that this oxide particle is not magnetite. Comparing the spectrum with the reference spectrum of ilmenite, a good agreement between these spectra was obtained. Hence, the hexagonal crystals forming on the surface was mainly ilmenite ($FeTiO_3$).

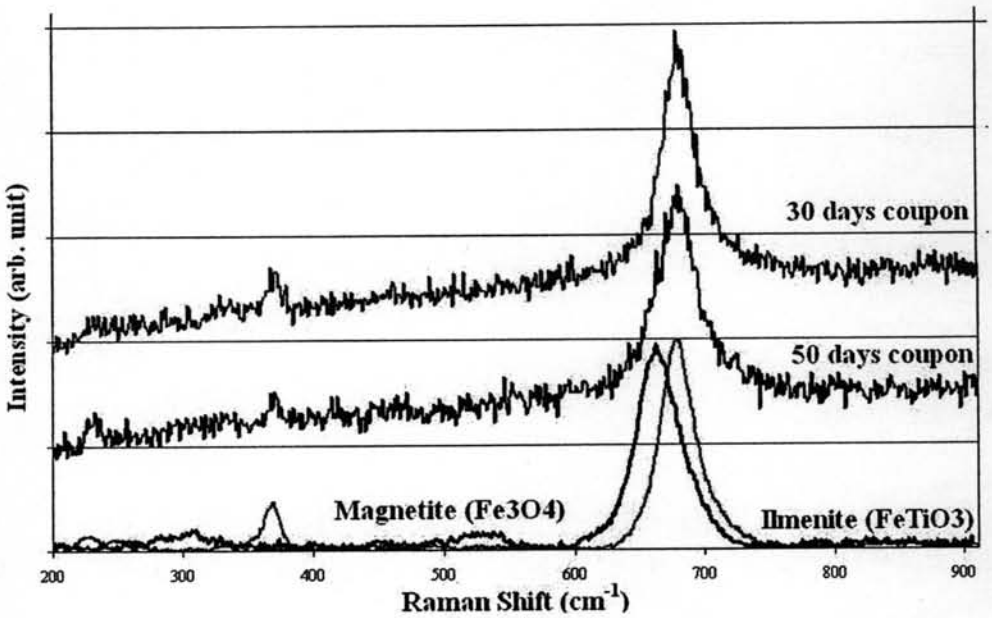

Figure 5.19 Raman spectra of hexagonal crystalline particles compared with the reference magnetite and ilmenite spectra.

The presence of titanium in the system is an important parameter which can affect the structure of oxide films formed on the metal surface. The standard Gibbs free energy of formation of ilmenite and magnetite are -1199.38 and -1015.36 kJ/mol, respectively (G.H. Kelsall *et al.*, 1990). Both oxide compounds can form spontaneously. However, due to the higher negative value of the standard Gibbs free energy of formation for ilmenite than that for magnetite, the crystalline particles prefer to form as ilmenite rather than magnetite (if there is titanium in the system). This is the reason why there is no magnetite crystalline particle found on the static sample surfaces. Another possible reason is about the solubility of each oxide particle. According to Bateman *et al.* (2002), ilmenite was less soluble than magnetite and therefore it would crystallize preferentially.